

Published in final edited form as:

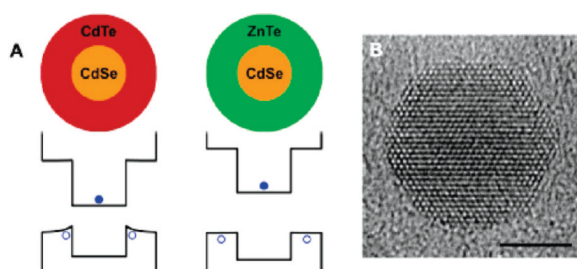
Acc Chem Res. 2010 February 16; 43(2): 190–200. doi:10.1021/ar9001069.

Semiconductor Nanocrystals: Structure, Properties, and Band Gap Engineering

ANDREW M. SMITH and SHUMING NIE*

Departments of Biomedical Engineering and Chemistry, Emory University and Georgia Institute of Technology, 101 Woodruff Circle, Suite 2001, Atlanta, Georgia 30322

Abstract



Semiconductor nanocrystals are tiny light-emitting particles on the nanometer scale. Researchers have studied these particles intensely and have developed them for broad applications in solar energy conversion, optoelectronic devices, molecular and cellular imaging, and ultrasensitive detection. A major feature of semiconductor nanocrystals is the quantum confinement effect, which leads to spatial enclosure of the electronic charge carriers within the nanocrystal. Because of this effect, researchers can use the size and shape of these “artificial atoms” to widely and precisely tune the energy of discrete electronic energy states and optical transitions. As a result, researchers can tune the light emission from these particles throughout the ultraviolet, visible, near-infrared, and mid-infrared spectral ranges. These particles also span the transition between small molecules and bulk crystals, instilling novel optical properties such as carrier multiplication, single-particle blinking, and spectral diffusion. In addition, semiconductor nanocrystals provide a versatile building block for developing complex nanostructures such as superlattices and multimodal agents for molecular imaging and targeted therapy.

In this Account, we discuss recent advances in the understanding of the atomic structure and optical properties of semiconductor nanocrystals. We also discuss new strategies for band gap and electronic wave function engineering to control the location of charge carriers. New methodologies such as alloying, doping, strain-tuning, and band-edge warping will likely play key roles in the further development of these particles for optoelectronic and biomedical applications.

I. Introduction

Semiconductor nanocrystals are tiny crystalline particles that exhibit size-dependent optical and electronic properties.^{1–3} With typical dimensions in the range of 1–100 nm, these nanocrystals bridge the gap between small molecules and large crystals, displaying discrete electronic transitions reminiscent of isolated atoms and molecules, as well as enabling the

exploitation of the useful properties of crystalline materials. Bulk semiconductors are characterized by a composition-dependent band gap energy (E_g), which is the minimum energy required to excite an electron from the ground state valence energy band into the vacant conduction energy band (Figure 1A). With the absorption of a photon of energy greater than E_g , the excitation of an electron leaves an orbital *hole* in the valence band. The negatively charged electron and positively charged hole may be mobilized in the presence of an electric field to yield a current, but their lowest energy state is an electrostatically bound electron-hole pair, known as the *exciton*. Relaxation of the excited electron back to the valence band annihilates the exciton and may be accompanied by the emission of a photon, a process known as *radiative recombination*.

The exciton has a finite size within the crystal defined by the Bohr exciton diameter (a_B), which can vary from 1 nm to more than 100 nm depending on the material. If the size of a semiconductor nanocrystal is smaller than the size of the exciton, the charge carriers become spatially confined, which raises their energy. Therefore, the exciton size delineates the transition between the regime of bulk crystal properties and the *quantum confinement* regime, in which the optical and electronic properties are dependent on the nanocrystal size. Nanocrystals with dimensions smaller than a_B demonstrate size-dependent absorption and fluorescence spectra with discrete electronic transitions.

Figure 1C displays these effects for quasi-spherical nanocrystals, showing that the wavelengths of fluorescence and absorption can be tuned by nanocrystal size. For example, nanocrystals composed of the prototypical material CdSe ($E_g = 1.76$ eV, $a_B = 9.6$ nm) can be tuned through quantum confinement to emit fluorescent light throughout the visible spectrum, making them useful for both biological imaging and many types of optoelectronic devices. In addition, the crystalline nature of these particles imparts a large density of electronic states, yielding giant extinction coefficients and broad absorption spectra that are unavailable from organic chromophores. State-of-the-art quantum dots have been engineered to have a quantum efficiency of radiative recombination approaching unity at room temperature, far above what has been achieved from bulk materials.^{4,5} This high efficiency of light emission is largely due to the strong overlap between the electron and hole wave functions in the confined structure, whereas the exciton in bulk semiconductors is not confined in space and can rapidly dissociate, increasing the probability of nonradiative relaxation events associated with crystalline defects and charge carrier traps on crystal surfaces.

Early studies on semiconductor nanocrystals made use of particles embedded in glass matrices, similar to centuries-old stained glass containing semiconductor crystallite pigments.⁶⁻⁸ Today, these nanocrystals are commonly fabricated as colloids suspended in solution or as epitaxial structures grown on solid crystalline substrates (Figure 1B). Epitaxial nanocrystals can be reproducibly prepared with a wide range of shapes and sizes in regular patterns and directly incorporated into optoelectronic devices. However, solution phase techniques provide exceptional control over size, monodispersity, and shape. These particles are typically coated with a monolayer of surfactants and have shown versatile applicability in optoelectronic devices and as biomolecular conjugates. As discussed the following sections, colloidal semiconductor nanocrystals have largely enabled the physical understanding of size-dependent properties and have catalyzed the broad use of nanometer-sized particles.

II. Nanocrystal Structure

Shape

The most important consequence of the quantum confinement effect is the size dependence of the band gap for nanocrystalline semiconductors. By confining the exciton of a semiconductor, the band gap may be tuned to a precise energy depending on the dimensionality and degree of confinement.⁹ Figure 2A depicts the shift of the band gap of CdSe nanocrystals confined in three dimensions (quantum dots), two dimensions (quantum wires or rods), or one dimension (quantum wells or disks). An increase in the number of confined dimensions yields a stronger degree of electronic confinement and thus a wider range of tunability in the band gap, although exceptions to this trend have been reported for CdTe nanocrystals.¹⁰ Quantum dots have attracted broad attention due to their wide optical tunability and utility for biolabeling, whereas elongated structures have been shown to emit linearly polarized light with a wide energy separation between the absorption and emission maxima (Stokes shift), which can reduce light reabsorption for light emission applications.¹¹ Quantum wells are well-established components of optoelectronic devices, and their colloidal “disk” analogues have recently been described,¹² which may have novel piezoelectric applications if they can be confined in polar lattice directions.

Surface Properties

The dependence of optical properties on particle size is largely a result of the internal structure of the nanocrystal. However, as the crystal becomes smaller, the number of atoms on the surface increases, which can also impact the optical properties. The atoms on the surface of a crystal facet are incompletely bonded within the crystal lattice, thus disrupting the crystalline periodicity and leaving one or more “dangling orbital” on each atom pointed outward from the crystal. Most nanocrystals are highly faceted (Figure 3A-C), and each surface contains a periodic array of *unpassivated* orbitals with two-dimensional translational symmetry, which may form a band structure similar to that of the three-dimensional crystal itself.^{15,16} If these surface energy states are within the semiconductor band gap, they can trap charge carriers at the surface, thereby reducing the overlap between the electron and hole, increasing the probability of nonradiative decay events. In practice, however, most semiconductor nanocrystals are not used in vacuum, but instead are either embedded within a solid matrix such as another crystal or a glass, or suspended in solution and coated with organic ligands such as trioctylphosphine oxide (TOPO) or hexadecylamine (HDA). Thereby, the dangling bonds on the exposed facets are *passivated* by bonding with atoms or molecules (Figure 3D), minimizing intraband gap surface states and reducing surface atomic reconstruction. For colloidal particle suspensions, molecules such as TOPO and HDA adsorb to the nanocrystal surface through dative ligand-metal bonds between the basic moiety on the ligand and metal atoms on the nanocrystal surface, solubilizing the crystal in nonpolar solvents through hydrophobic interactions with the alkyl chains on the ligands.¹⁷ Polar end groups and hydrophilic polymers may be similarly used to solubilize nanocrystals in polar solvents.

The fluorescence emission can be significantly modulated by alterations to the nanocrystal surface. For example, very small colloidal CdSe nanocrystals often display two fluorescence emission bands, one at the band edge and another at lower energy resulting from recombination at intraband gap defect sites on the surface (Figure 3E).¹⁶ Deep trap emission arises from the presence of Se²⁻-rich facets, which poorly bind to most basic ligands, making these nanocrystals especially prone to surface trapping of holes which primarily reside on the selenium sp³ orbitals.¹⁶ Indeed, nanocrystals with surfaces terminated mostly by anions typically have little or no fluorescence emission due to the overwhelming number of surface trap states for nonradiative recombination. The addition of excess Cd²⁺ ions can

passivate these selenium states, yielding cationic surfaces that can strongly bind to basic ligands, and electrostatically shield holes from surface traps. Surface modifications may also introduce defects on the nanocrystal surface. Small amounts of oxidizing agents such as hypochlorous acid or hydrogen peroxide can etch away fragments of the nanocrystal surface, leaving behind unpassivated orbitals and atomic vacancies, nearly extinguishing the fluorescence with as little as 10 hypochlorous acid molecules per nanocrystal.¹⁸

The number of surface atoms and the types of facets are also dictated by the nanocrystal shape. Figure 2B shows the fraction of surface atoms on a CdSe nanocrystal for different shapes and sizes. Spherical quantum dots have the smallest number of total surface atoms and are thermodynamically the most stable, thus making them ideal candidates for applications in which fluorescence modulation from external stimuli must be minimized. On the other hand, elongated structures such as rods and wires maintain a large fraction of their constituent atoms on their surfaces, making them useful for applications in which the nanocrystal charge carriers can interact with the surrounding environment, such as for redox chemistry, energy transfer, photocatalysis, and sensing applications. However, it should be noted that, for nanocrystals of the same volume, the diffusive kinetics decrease much faster for elongated structures, which may detrimentally impact sensing applications in viscous media. Several other interesting materials properties are closely linked with the fraction of surface atoms on the nanocrystal. The melting temperature of nanocrystals decreases as the size decreases, as a larger fraction of atoms of the crystal are on the disordered, incompletely passivated surface.³ The surface energy differences between different crystal phases have also been used to explain alterations to the pressure-induced phase transitions in high-surface-area semiconductor nanocrystals relative to their bulk counterparts.¹⁹

Shell Passivation

For practical light-emitting applications, it is advantageous to coat semiconductor nanocrystals with an insulating inorganic shell in order to stabilize and maximize fluorescence. This not only passivates the surface bonds but also buries the semiconductor in a potential energy well, concentrating the charge carriers in the nanocrystal core, away from the surface.^{5,20,21} Thereby, surface defect states and trap sites will have a diminished impact on the fluorescence efficiency and fewer environmental factors will influence the emission intensity. In solid state devices, this process is quite simple, as overgrowth of an inorganic layer with a wider band gap can be readily achieved with complete surface coverage. In colloids, the task is more challenging, but major progress has resulted in colloidal (core)shell quantum dots such as (CdSe)ZnS and (CdSe)CdS with efficient and stable fluorescence. Wider band gap CdS and ZnS shells not only electronically insulate the cores, but S^{2-} has a much lower oxidation potential than Se^{2-} , resulting in a higher threshold to photo-oxidative degradation and surface defect formation. In addition, the implementation of shells composed of elements with smaller atomic radii is crucial for ligand binding, as a higher packing density of organic ligands can enhance colloidal stability and create a steric barrier to degradative small molecules.

III. Optical Properties

Unlike solid state crystals and small-molecule chromophores and fluorophores, quantum confined semiconductor structures exhibit unique optical properties dictated by their structure and size. One of the most striking features is the random on-and-off blinking phenomenon exhibited by single particles. In addition, illumination at high energies may result in the production of many charge carriers in a single particle, which may increase the efficiency of photovoltaic and light-emitting devices.

On/Off Blinking

The emission from single quantum dots is intermittent (blinking), similar to effects that have also been observed for fluorescent dyes and proteins.^{22,23} This provides an “elegant” means to identify single, isolated quantum dots, although this behavior has resulted in problems for tracking the motion of particles in biological environments due to the repeated loss of signal. The light emission efficiency from a single quantum dot is thought to be quantized, with near-unity fluorescence efficiency in the bright state and zero emission in the dark state, while occasionally observed intermediate luminescent intensity levels are believed to result from insufficient temporal resolution. In the dark state, quantum dots still absorb light at the same rate, and within each ensemble some quantum dots are permanently dark. Several reports have shown a correlation between the ensemble quantum yield and number of dark particles, with highly efficient batches showing fewer dark particles and a high probability of bright states for blinking particles.^{24,25} The blinking phenomenon is thought to arise from either repeated ionization of the nanocrystal due to an Auger process or from trapping of one of the charge carriers at or near the particle surface (Figure 4). In accord with these theories, the off time can be reduced in low dielectric media that poorly solvate an expelled charge, and through the adsorption of thiolate ligands and amines, which can neutralize surface traps for charge carriers.²⁶ In addition, growing an insulating shell around the nanocrystal to yield a deeper and wider potential well has been shown to significantly decrease the off time of the nanocrystal. In fact, the groups of Dubertret and Hollingsworth have recently shown that colloidal (CdSe)CdS quantum dots with thick insulating shells are nearly nonblinking, resembling self-assembled quantum dots embedded in crystalline substrates (Figure 4).^{27,28} In addition, Krauss and co-workers have demonstrated that blinking can be eliminated in (core)shell structures in which there is a smooth composition gradient from the core to the shell.²⁹ The key concept is that more gradual changes in the confinement potential prevent Auger recombination, permitting fluorescence emission even from ionized nanocrystals (see Figure 4). However, the exact structure of these nonblinking nanocrystals and their light emission mechanisms need to be further investigated.

Carrier Multiplication

Another intriguing and valuable attribute of quantum dots is carrier multiplication.^{30,31} When a quantum dot is excited by a photon with an energy at least twice its band gap, the electron and hole that result may release their excess kinetic energy through the excitation of a second electron in a collision-like Auger process, resulting in a biexciton and an internal quantum efficiency greater than 100% (Figure 5). Thereby, excess kinetic energy is no longer dissipated into lattice vibrations, which may yield improved efficiencies in photovoltaic devices. These Auger processes are efficient in nanocrystals compared to their bulk counterparts due to suppression of the phonon-assisted decay rate and the large energy separations between electronic energy levels.³² However, because Auger processes are so fast, subsequent Auger processes may eliminate the excess excitons, such that they do not have time to radiatively recombine. In fact, ultrafast pump-probe spectroscopies must be employed to observe the formation and recombination of multiexciton states. Recently, biexciton and triexciton fluorescence has been observed at room temperature with high quantum efficiency (11% and 5%, respectively) and long lifetimes (790 ps for the biexciton) in highly luminescent (CdSe)ZnS quantum dots.³³ The current challenge is to harness these extra charge carriers by maximizing their stabilization before they decay via Auger processes to convert them into an external electric current, perhaps through implementation of a weakly coupled multilayer structure in which the excitons can segregate, as charge transfer in semiconductor nanocrystals generally occurs much faster (~500 fs) than Auger processes.³⁴

IV. Band Gap and Wave Function Engineering

In comparison with bulk semiconductors, nanocrystals have a diverse and growing range of parameters that can modulate their electronic band gaps (Figure 6) including size, shape, and composition. Quantum confinement can shift the band gap of most semiconductors by over 1 eV, giving an enormous range of continuous tunability through size and shape for a single material composition. The use of quantum confined structures also allows the independent tuning of size and band gap through the implementation of homogeneously alloyed materials such as $\text{CdSe}_y\text{Te}_{1-y}$, and $\text{Cd}_x\text{Zn}_{1-x}\text{S}$.^{35,36} A chemically related process to alloying is impurity doping, which creates an intraband electronic energy level that allows lower energy light emission from the defect state to the ground state. Doped nanocrystals can have interesting properties for biolabeling and device applications, such as large Stokes shifts, paramagnetic properties, and improved lasing. At the present, however, the synthesis of these doped nanocrystals is still a challenge due to the chemical dissimilarities between the dopants and their crystalline matrices.³⁷ More recently, the manipulation of nanocrystal heterostructures has given rise to complex control over charge carrier wave functions, resulting in new optical properties.

Type-II Quantum Dots

In 2003, Bawendi and co-workers developed (core)shell semiconductor heterostructures in which the conduction and valence bands of the core and shell material are staggered, resulting in the segregation of the electron and the hole between the core and shell materials.³⁸ For example, (core)shell (CdTe)CdSe particles have a minimum conduction band energy in the CdSe shell, whereas the maximum energy of the valence band is in the CdTe core (Figure 6). These energy band offsets segregate the electron to the shell and the hole to the core, and carrier recombination can occur across the interface at a lower energy than the band gaps of either of the constituent semiconductor materials. During the course of shell growth, the wavelength of emission shifts strongly to the red, adding a new dimension to band gap engineering. The reduced spatial overlap between the electron and hole also results in a major reduction in band edge oscillator strength and a significant increase in excited state lifetimes. This band alignment is designated as “type-II” in order to distinguish it from “type-I” band alignments like those of (CdSe)ZnS in which the electron and hole overlap in space in the core material. Type-II materials may be greatly beneficial for photovoltaic devices, especially with the development of anisotropic materials in which the segregation of charges is directional, which may enhance directional charge transport in future electronic devices.³⁹ The use of type-II nanocrystals is also a means by which to independently control which charge carrier is accessible to the surface for charge transfer applications. It is also possible to sequester both charge carriers in the shell material in inverted type-I alignments, which resemble a quantum well in which one-dimensional confinement is present in the radial direction. The capacity to transition between core and shell localization has recently been exploited by Klimov and co-workers to tune the interactions between charge carriers and core-localized magnetic atoms of (ZnSe:Mn)CdSe quantum dots.⁴⁰

Strain Tuning

Semiconductor nanocrystals are greatly impacted by the effects of strain in both the solid state phase and the colloidal state. Lattice strain is the reason that islands of quantum dots spontaneously grow on lattice mismatched solid substrates in the Stranski-Krastanov growth mode, leaving substantial residual strain in the nanocrystals. Colloidal semiconductor quantum dots such as (CdSe)ZnS (core)shell materials have a large mismatch in bond length between the core and shell materials (12%), generating a strain field in the nanocrystal. In both solid-phase fabrication and colloidal chemical synthesis, growth of a material on a substrate with a different bond length can only proceed to a *critical thickness* before a lattice

defect (commonly a misfit dislocation) will arise near the interface to ease the strain, allowing the materials to relax to their native bond lengths and introducing carrier traps in the process (Figure 7A). However, colloidal nanocrystals behave differently from those fabricated on solid substrates, because, unlike large crystals, an isolated nanocrystal can deform to adapt to the overgrowth of a straining shell and the large surface area allows the stress to be distributed over a large fraction of the constituent atoms. Deformation of a semiconductor forces the material to adopt an unnatural bond length. Because the energies of the conduction and valence band edges derive from the bond strength in the crystal, changes in the bond length alter the electronic band gap. This change is described by the deformation potential, α , defined as

$$\alpha = \frac{\partial E_g}{\partial (\ln V)}$$

where $\partial (\ln V)$ is the fractional volume change. For II-VI and III-V materials, α is negative ($\alpha_{\text{CdSe}} = -2.9$), meaning that compression of the crystal widens the band gap (Figure 7B). This effect can be observed directly using a diamond anvil cell on a bulk crystal, demonstrating a linear relationship between the band gap and pressure, which also holds true for nanocrystals of semiconductors.¹⁹

A recent report has highlighted the unique role of strain in colloidal (core)shell quantum dot heterostructures.⁴¹ For nanocrystal cores smaller than a specific size, the critical thickness for a particular shell is theoretically infinite, allowing any thickness of shell without the introduction of lattice-relaxing defects. For example, the bond length difference between CdTe ($a = 6.482 \text{ \AA}$) and CdS (5.818 \AA) is 11.4%, but CdTe cores smaller than 4 nm can tolerate the growth of any CdS shell thickness purely through coherent growth without defect formation. Thus, if the materials composing the heterostructure are reasonably deformable, strain can be tolerated and shared across the entire nanoparticle without the introduction of quenching defects. Because such heterostructures can be grown coherently as a single crystalline domain, homogeneous lattice strain results in significant bond length alterations that can modify electronic band energies. Compressive strain will shift both the conduction and valence bands to higher energy, and tensile strain will shift the bands to lower energy. Thereby, the coherent growth of compressive shells (e.g., ZnSe or CdS) on CdTe core colloids yields dramatic changes to the relative energy bands in the heterostructure, resulting in type-II band alignments with widely tunable band gaps for these normally type-I heterostructures (Figure 8). This effect is also believed to increase the type-II nature of strained heterostructures such as (CdTe)CdSe that are already type-II in bulk. For this type of band gap engineering, an important component is the implementation of CdTe nanocrystal cores. Compared to the more commonly studied CdSe, CdTe is softer, has a larger deformation potential, and has a much larger difference in lattice constant compared to common shell materials (e.g., ZnS, CdS). Materials with similar properties, such as the III-V antimonides and the other II-VI tellurides, are predicted to have similar attributes.

Strain also plays a critical role in warping (or bending) charge carrier wave functions at heterostructural interfaces. Because the strain field in a lattice-mismatched (core)shell quantum dot is inhomogeneous in the shell, the band edge is believed to deform over the radial direction, giving rise to inhomogeneous charge carrier distributions. This is likely the cause of the different fluorescence behaviors of (CdSe)CdTe and (CdSe)ZnTe nanocrystals. Both of these heterostructures are type-II with the hole sequestered in the shell and the electron in the core, but heterostructures with CdTe shells have quantum yields (20-40%) dramatically larger than that (<1%) with ZnTe shells. It is important to realize that the lattice mismatch between CdSe and CdTe is 7%, whereas the lattice mismatch is only 0.6% for

ZnTe. The high strain in the CdTe shell will shift the hole wave function toward the core material (Figure 9), increasing the overlap between the electron and hole and thus the probability of carrier recombination. The near absence of strain for ZnTe shells substantially increases the wave function localization at the nanocrystal surface, where surface traps increase the probability of nonradiative relaxation. Indeed, in true unstrained type-II band alignments, the probability of band-edge recombination efficiency should be very low, and engineering the strain in such heterostructures may be important for modulating recombination versus carrier separation. Inhomogeneous strain fields in shells have also been proposed as the means by which Mn^{2+} dopant energy levels can be continuously tuned in the shells of (CdS)/ZnS nanocrystals.⁴²

V. Concluding Remarks

Looking into the future, we expect major advances in both fundamental studies and practical applications for semiconductor nanocrystals. For fundamental research, the synthesis of new nanocrystals with unusual structures and properties is a boundless frontier and will continue to yield surprises such as doped and strain-tuned quantum dots. Through single-particle fluorescence,²⁶ extinction,⁴³ and tunneling spectroscopies⁴⁴ as well as ultrafast spectroscopies,⁴⁵ it is possible that complex electronic states (such as defect and surface states) could soon be understood for various types of semiconductor nanocrystals. There are also a wide variety of new nanocrystalline materials available with a diverse range of chemical, elastic, and optical properties. In particular, oxide materials such as ZnO would be an exceptional shell material for nanocrystal capping due to a wide band gap and resistance to oxidative degradation; IV-VI semiconductors have uniquely positive deformation potentials; and mercury-based II-VI materials may allow the continuous tuning of band gaps through spontaneous cation exchange reactions. For photovoltaic applications, it will be important to engineer nanocrystals for multiexciton generation and efficient charge carrier separation. For biomedical applications, it is important to minimize the overall size of bioconjugated nanocrystals, to reduce steric hindrance and nonspecific protein adsorption, to develop chemically activatable or photoswitchable nanocrystals for multicolor super-resolution optical microscopy, and to understand the potential toxic effects of semiconductor materials.⁴⁶

Acknowledgments

This work was supported by grants from the U.S. National Institutes of Health (P20 GM072069, R01 CA108468, U01HL080711, U54CA119338, and PN2EY018244). A.M.S. acknowledges the Whitaker Foundation for generous fellowship support, and S.M.N is a Distinguished Scholar of the Georgia Cancer Coalition (GCC).

Biography

Andrew M. Smith is a Distinguished Fellow of the NIH Center for Cancer Nanotechnology Excellence at Emory University. He received his B.S. degree in Chemistry and his Ph.D. in Bioengineering, both from the Georgia Institute of Technology. His research focuses on nanomaterials engineering for molecular imaging of cancer and the exploration of the interactions between nanostructures and biological systems.

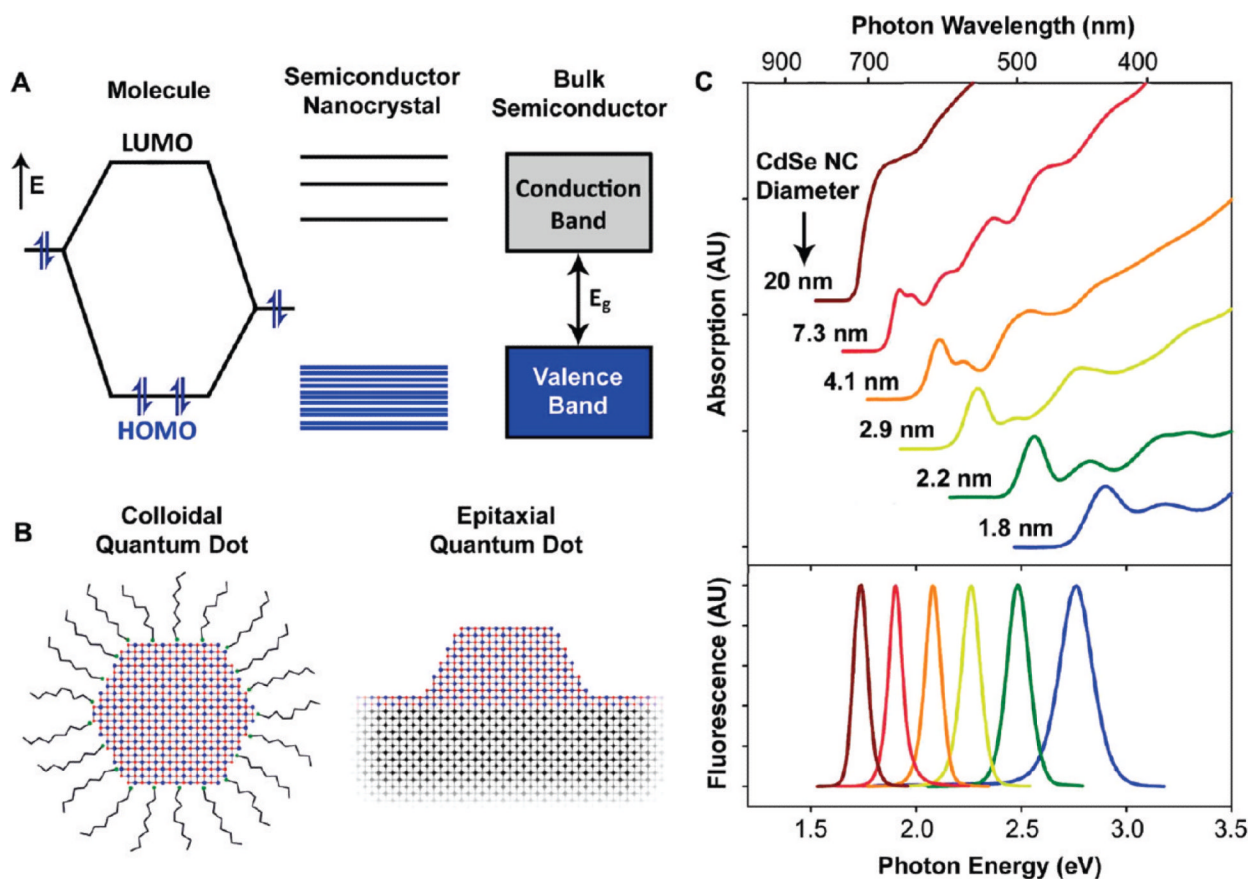
Shuming Nie is the Wallace H. Coulter Distinguished Chair Professor of Biomedical Engineering at Emory University and Georgia Institute of Technology. He received his B.S. degree from Nankai University and his M.S. and Ph.D. degrees from Northwestern University, and did his postdoctoral training at both Georgia Tech and Stanford University. His research interests are primarily in the areas of biomolecular engineering and nanotechnology, with a focus on bioconjugated nanoparticles for molecular imaging, molecular profiling, pharmacogenomics, and targeted therapy.

REFERENCES

1. Brus LE. Electron-electron and electron-hole interactions in small semiconductor crystallites - the size dependence of the lowest excited electronic state. *J. Chem. Phys* 1984;80:4403–4409.
2. Bawendi MG, Steigerwald ML, Brus LE. The quantum mechanics of larger semiconductor clusters (“quantum dots”). *Annu. Rev. Phys. Chem* 1990;41:477–496.
3. Alivisatos AP. Perspectives on the physical chemistry of semiconductor nanocrystals. *J. Phys. Chem* 1996;100:13226–13239.
4. Nirmal M, Brus L. Luminescence photophysics in semiconductor nanocrystals. *Acc. Chem. Res* 1999;32:407–414.
5. McBride J, Treadway J, Feldman LC, Pennycook SJ, Rosenthal SJ. Structural basis for near unity quantum yield core/shell nanostructures. *Nano Lett* 2006;6:1496–1501. [PubMed: 16834437]
6. Ekimov AI, Onushchenko AA. Quantum size effect in the optical-spectra of semiconductor microcrystals. *Sov. Phys. Semicond* 1982;16:775–778.
7. Warnock J, Awschalom DD. Quantum size effects in simple colored glass. *Phys. Rev. B* 1985;32:5529–5531.
8. Borrelli NF, Hall DW, Holland HJ, Smith DW. Quantum confinement effects of semiconducting microcrystallites in glass. *J. Appl. Phys* 1987;61:5398–5409.
9. Buhro WE, Colvin VL. Semiconductor nanocrystals - Shape matters. *Nat. Mater* 2003;2:138–139. [PubMed: 12612665]
10. Sun JW, Wang LW, Buhro WE. Synthesis of cadmium telluride quantum wires and the similarity of their effective band gaps to those of equidiameter cadmium telluride quantum dots. *J. Am. Chem. Soc* 2008;130:7997–8005. [PubMed: 18507463]
11. Scher EC, Manna L, Alivisatos AP. Shape control and applications of nanocrystals. *Philos. Trans. R. Soc. London, Ser. A* 2003;361:241–255.
12. Ithurria S, Dubertret B. Quasi 2D colloidal CdSe platelets with thicknesses controlled at the atomic level. *J. Am. Chem. Soc* 2008;130:16504–16505. [PubMed: 19554725]
13. Peng XG. Mechanisms for the shape-control and shape-evolution of colloidal semiconductor nanocrystals. *Adv. Mater* 2003;15:459–463.
14. Manna L, Milliron DJ, Meisel A, Scher EC, Alivisatos AP. Controlled growth of tetrapod-branched inorganic nanocrystals. *Nat. Mater* 2003;2:382–385. [PubMed: 12764357]
15. Pokrant S, Whaley KB. Tight-binding studies of surface effects on electronic structure of CdSe nanocrystals: the role of organic ligands, surface reconstruction, and inorganic capping shells. *Eur. Phys. J. D* 1999;6:255–267.
16. Underwood DF, Kippeny T, Rosenthal SJ. Ultrafast carrier dynamics in CdSe nanocrystals determined by femtosecond fluorescence upconversion spectroscopy. *J. Phys. Chem. B* 2001;105:436–443.
17. Murray CB, Norris DJ, Bawendi MG. Synthesis and characterization of nearly monodisperse CdE (E = S, Se, Te) semiconductor nanocrystallites. *J. Am. Chem. Soc* 1993;115:8706–8715.
18. Mancini MC, Kairdolf BA, Smith AM, Nie SM. Oxidative quenching and degradation of polymer-encapsulated quantum dots: new insights into the long-term fate and toxicity of nanocrystals in vivo. *J. Am. Chem. Soc* 2008;130:10836–10837. [PubMed: 18652463]
19. Tolbert SH, Alivisatos AP. High-pressure structural transformations in semiconductor nanocrystals. *Annu. Rev. Phys. Chem* 1995;46:595–625.
20. Dabbousi BO, Rodriguez-Viejo J, Mikulec FV, Heine JR, Mattoussi H, Ober R, Jensen KF, Bawendi MG. (CdSe)ZnS core-shell quantum dots: Synthesis and characterization of a size series of highly luminescent nanocrystallites. *J. Phys. Chem. B* 1997;101:9463–9475.
21. Hines MA, Guyot-Sionnest P. Synthesis and characterization of strongly luminescing ZnS-capped CdSe nanocrystals. *J. Phys. Chem* 1996;100:468–471.
22. Nirmal M, Dabbousi BO, Bawendi M, Macklin JJ, Trautman JK, Harris TD, Brus LE. Fluorescence intermittency in single cadmium selenide nanocrystals. *Nature* 1996;383:802–804.
23. Empedocles SA, Bawendi M. Spectroscopy of single CdSe nanocrystallites. *Acc. Chem. Res* 1999;32:389–396.

24. Yao J, Larson DR, Vishwasrao HD, Zipfel WR, Webb WW. Blinking and nonradiant dark fraction of water-soluble quantum dots in aqueous solution. *Proc. Natl. Acad. Sci. U.S.A* 2005;102:14284–14289. [PubMed: 16169907]
25. Ebenstein Y, Mokari T, Banin U. Fluorescence quantum yield of CdSe/ZnS nanocrystals investigated by correlated atomic-force and single-particle fluorescence microscopy. *Appl. Phys. Lett* 2002;80:4033–4035.
26. Gomez DE, Califano M, Mulvaney P. Optical properties of single semiconductor nanocrystals. *Phys. Chem. Chem. Phys* 2006;8:4989–5011. [PubMed: 17091151]
27. Mahler B, Spinicelli P, Buil S, Quelin X, Hermier JP, Dubertret B. Towards non-blinking colloidal quantum dots. *Nat. Mater* 2008;7:659–664. [PubMed: 18568030]
28. Chen YF, Vela J, Htoon H, Casson JL, Werder DJ, Bussian DA, Klimov VI, Hollingsworth JA. “Giant” multishell CdSe nanocrystal quantum dots with suppressed blinking. *J. Am. Chem. Soc* 2008;130:5026–5027. [PubMed: 18355011]
29. Wang X, Ren X, Hahn MA, Raheswaran S, Maccagnano-Zacher S, Silcox J, Cragg GE, Efros AL, Krauss TD. Non-blinking semiconductor nanocrystals. *Nature* 2009;459:686–689. [PubMed: 19430463]
30. Klimov VI. Spectral and dynamical properties of multilexcitons in semiconductor nanocrystals. *Annu. Rev. Phys. Chem* 2007;58:635–673. [PubMed: 17163837]
31. Klimov VI, Mikhailovsky AA, McBranch DW, Leatherdale CA, Bawendi MG. Quantization of multiparticle Auger rates in semiconductor quantum dots. *Science* 2000;287:1011–1013. [PubMed: 10669406]
32. Luo JW, Franceschetti A, Zunger A. Carrier multiplication in semiconductor nanocrystals: theoretical screening of candidate materials based on band-structure effects. *Nano Lett* 2008;8:3174–3181. [PubMed: 18729418]
33. Fisher B, Caruge JM, Zehnder D, Bawendi M. Room-temperature ordered photon emission from multiexciton states in single CdSe core-shell nanocrystals. *Phys. Rev. Lett* 2005;94:087403. [PubMed: 15783930]
34. Dooley CJ, Dimitrov SD, Fiebig T. Ultrafast electron transfer dynamics in CdSe/CdTe donor-acceptor nanorods. *J. Phys. Chem. C* 2008;112:12074–12076.
35. Bailey RE, Nie SM. Alloyed semiconductor quantum dots: Tuning the optical properties without changing the particle size. *J. Am. Chem. Soc* 2003;125:7100–7106. [PubMed: 12783563]
36. Zhong XH, Feng YY, Knoll W, Han MY. Alloyed $\text{Zn}_x\text{Cd}_{1-x}\text{S}$ nanocrystals with highly narrow luminescence spectral width. *J. Am. Chem. Soc* 2003;125:13559–13563. [PubMed: 14583053]
37. Erwin SC, Zu L, Haftel MI, Efros AL, Kennedy TA, Norris DJ. Doping semiconductor nanocrystals. *Nature* 2005;436:91–94. [PubMed: 16001066]
38. Kim S, Fisher B, Eisler HJ, Bawendi M. Type-II quantum dots: CdTe/CdSe(core/shell) and CdSe/ZnTe(core/shell) heterostructures. *J. Am. Chem. Soc* 2003;125:11466–11467. [PubMed: 13129327]
39. Kumar S, Jones M, Lo SS, Scholes GD. Nanorod heterostructures showing photoinduced charge separation. *Small* 2007;3:1633–1639. [PubMed: 17705316]
40. Bussian DA, Crooker SA, Yin M, Brynda M, Efros AL, Klimov VI. Tunable magnetic exchange interactions in manganese-doped inverted core-shell ZnSe–CdSe nanocrystals. *Nat. Mater* 2009;8:35–40. [PubMed: 19079242]
41. Smith AM, Mohs AM, Nie SM. Tuning the optical and electronic properties of colloidal nanocrystals by lattice strain. *Nat. Nanotechnol* 2009;4:56–63. [PubMed: 19119284]
42. Ithurria S, Guyot-Sionnest P, Mahler B, Dubertret B. Mn^{2+} as a radial pressure gauge in colloidal core/shell nanocrystals. *Phys. Rev. Lett* 2007;99:265501. [PubMed: 18233588]
43. Kukura P, Celebrano M, Renn A, Sandoghdar V. Imaging a single quantum dot when it is dark. *Nano Lett* 2009;9:926–929. [PubMed: 18671437]
44. Steiner D, Dorfs D, Banin U, Sala FD, Manna L, Millo O. Determination of band offsets in heterostructured colloidal nanorods using scanning tunneling spectroscopy. *Nano Lett* 2008;8:2954–2958. [PubMed: 18690751]
45. Klimov VI. Optical nonlinearities and ultrafast carrier dynamics in semiconductor nanocrystals. *J. Phys. Chem. B* 2000;104:6112–6123.

46. Smith AM, Duan HW, Mohs AM, Nie SM. Bioconjugated quantum dots for in vivo molecular and cellular imaging. *Adv. Drug Delivery Rev* 2008;60:1226–1240.

**FIGURE 1.**

(A) Electronic energy states of a semiconductor in the transition from discrete molecules to nanosized crystals and bulk crystals. Blue shading denotes ground state electron occupation. (B) Comparison of a colloidal quantum dot and an islandlike, self-assembled quantum dot epitaxially deposited on a crystalline substrate. (C) Absorption (upper) and fluorescence (lower) spectra of CdSe semiconductor nanocrystals showing quantum confinement and size tunability. AU = arbitrary units.

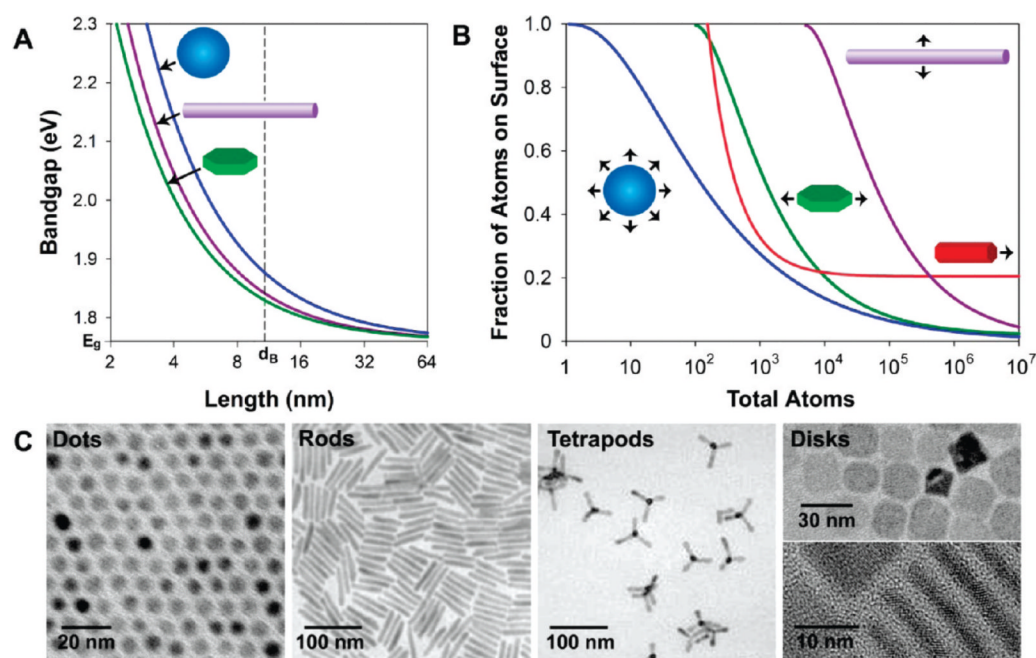
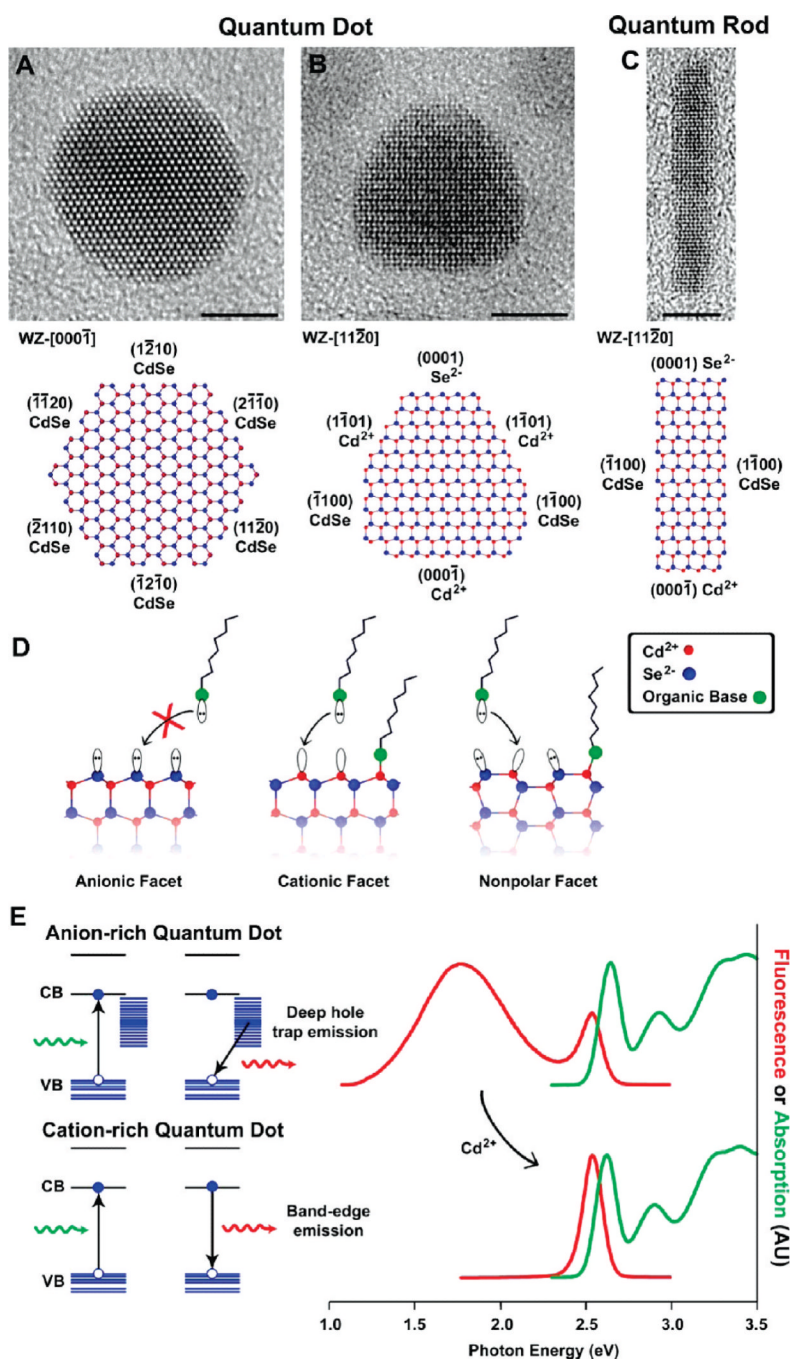
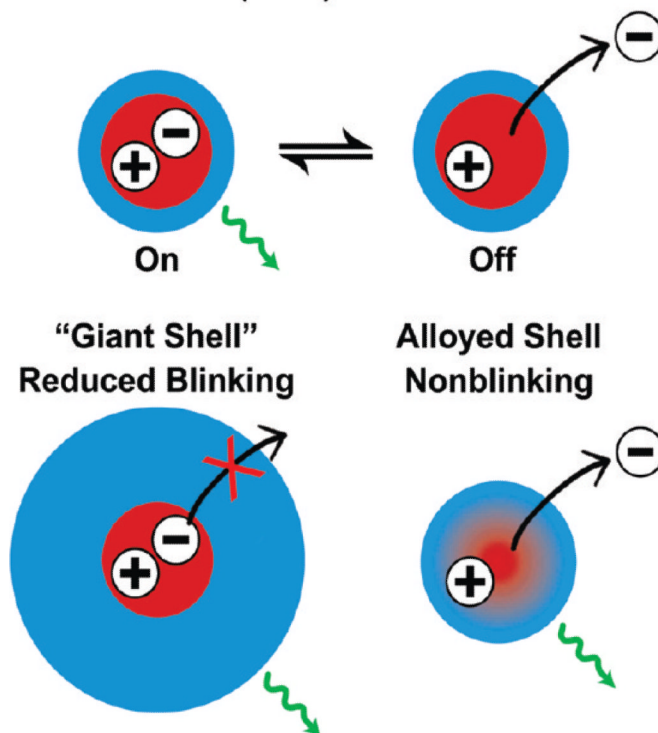


FIGURE 2.

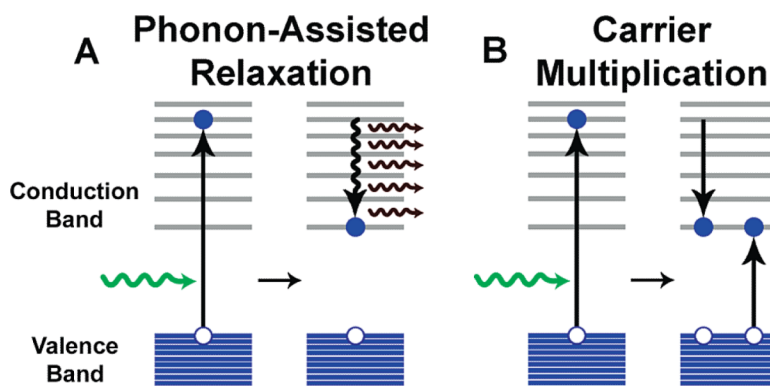
Impact of shape on the electronic and surface properties of semiconductor nanocrystals. (A) Band gaps of CdSe quantum wells, wires, and dots are plotted against the length of the confined dimension. The bulk band gap and exciton diameter are noted on the axes. (B) Fractions of atoms on the nanocrystal surface are plotted against the total number of atoms. The wires (purple) are $1\ \mu\text{m}$ in length, the disks (green) are 20 nm in length, and the rods (red) are 4 nm in diameter. (C) Transmission electron micrographs depicting CdSe dots,¹³ rods,¹³ tetrapods,¹⁴ and disks.¹²

**FIGURE 3.**

Surface properties of CdSe nanocrystals. Panels (A) and (B) depict transmission electron micrographs of quasi-spherical quantum dots with two orientations on the substrate, and panel (C) depicts a quantum rod.¹¹ All scale bars are 5 nm. In the atomic models, the crystalline orientations and lattice facets are identified by their Wurtzite (WZ) Miller indices, and the polarity of each facet is noted as Cd $^{2+}$ for cationic, Se $^{2-}$ for anionic, and CdSe for nonpolar. Panel (D) illustrates the terminal dangling orbitals on each type of facet, and panel (E) shows the effects of surface hole traps on the fluorescence of small 2.1 nm nanocrystals.

Conventional (Core)Shell Quantum Dots**FIGURE 4.**

Schematic diagrams showing on/off light emission (blinking) in conventional (core)shell nanocrystals (upper), and suppression of blinking in giant-shell and gradient alloy nanocrystals (lower). See text for discussion.

**FIGURE 5.**

Schematic illustration of electronic energy relaxation and carrier multiplication in quantum dots. (A) Electrons excited to energies greater than the band edge efficiently relax to the band edge through the release of phonons, or quanta of lattice vibration. (B) Alternatively, excited state electrons with kinetic energy greater than the band gap can transfer their energy to a second electron via impact ionization, yielding two excitons.

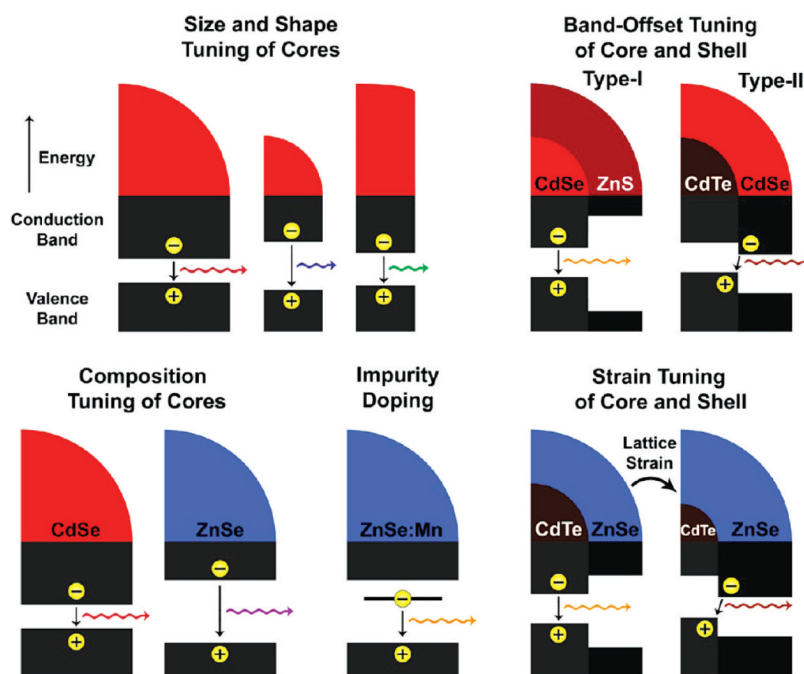
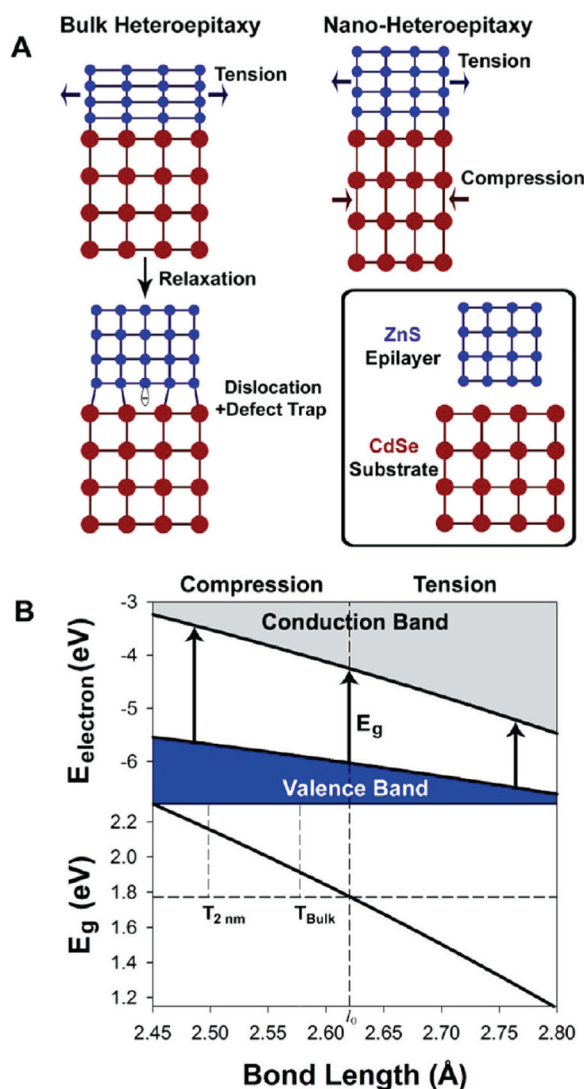
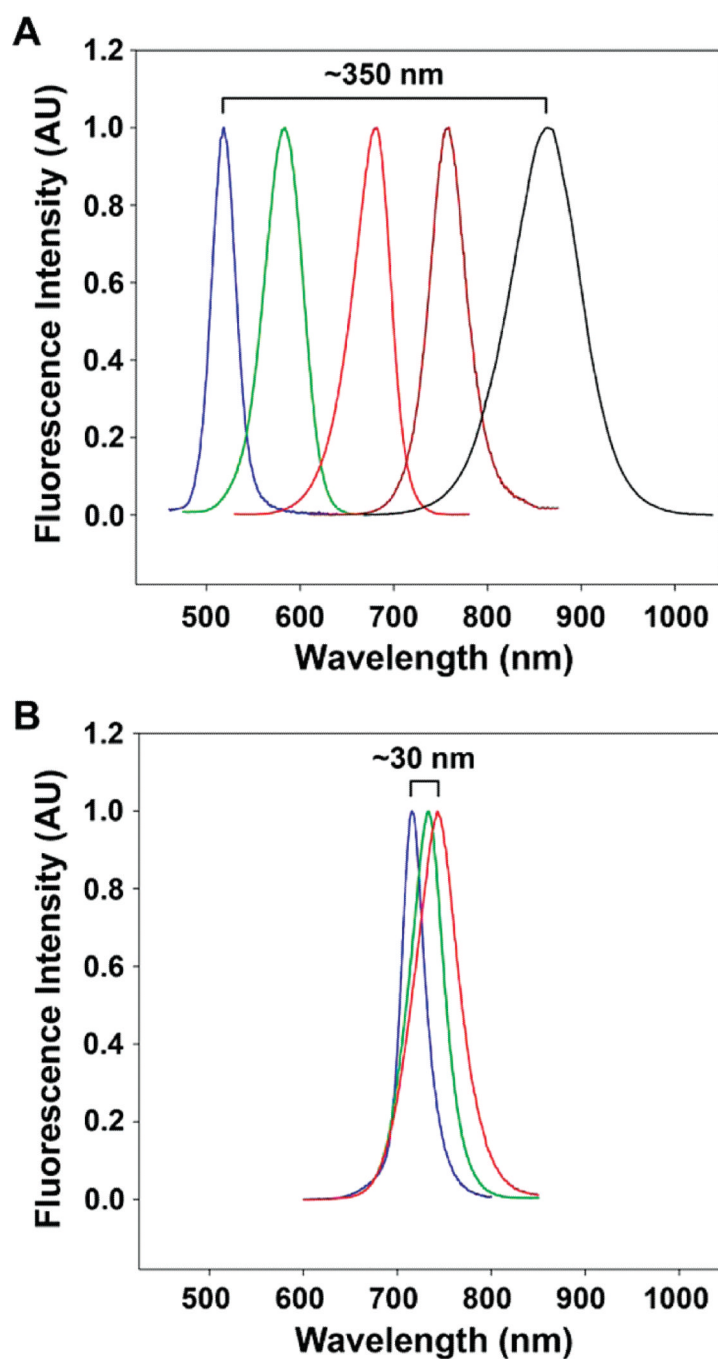


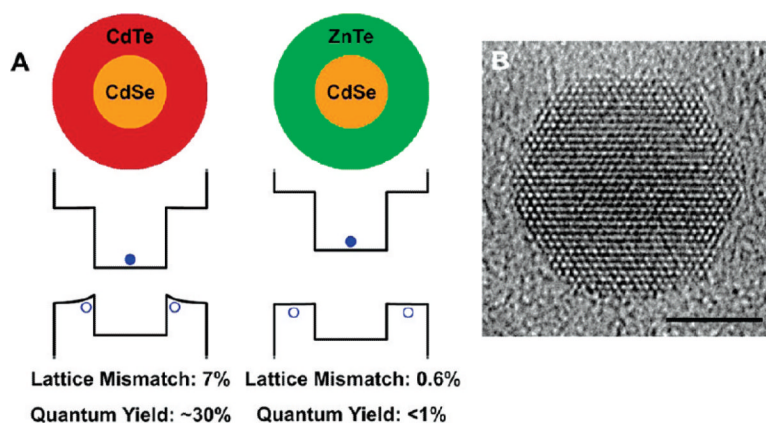
FIGURE 6. Mechanisms of band gap engineering in semiconductor nanocrystals through size, shape, composition, impurity doping, heterostructure band offset, and lattice strain. See text for discussion.

**FIGURE 7.**

Epitaxial semiconductor heterostructures and impact of strain on band gap energy. Panel (A) shows exaggerated crystal domains of CdSe and ZnS with a large mismatch in lattice constant. Epitaxial growth of ZnS on a bulk CdSe substrate results in tensile strain in ZnS that cannot be tolerated, resulting in relaxation of the tension through a misfit dislocation. However, a nanometer-sized CdSe substrate can deform with growth of a ZnS shell, resulting in a sharing of the strain through compression of the CdSe domain, preventing defect formation. Panel (B) depicts how the energy of the valence band edge, conduction band edge, and band gap change with CdSe bond length. The equilibrium bond length is noted on the x-axis ($l_0 = 2.62 \text{ \AA}$) in addition to the bond length that results in a phase transition in bulk (T_{Bulk}) and for small 2 nm nanocrystals ($T_{2\text{nm}}$).

**FIGURE 8.**

Fluorescence spectra of strain-tunable (CdTe)ZnSe quantum dots. (A) Fluorescence from 1.8 nm CdTe cores strongly red-shifts when capped with 0-6 monolayers of ZnSe shell (from blue to black) due to strain-induced changes in the core and shell lattices. (B) Fluorescence from 6.2 nm CdTe cores only exhibits a small red-shift when capped with 0-5 monolayers of ZnSe shell (from blue to red) due to strain relaxation through lattice defect formation. See ref ⁴¹.

**FIGURE 9.**

Band-edge warping induced by lattice strain. (A) Energy band levels of quantum confined, strained (core)shell (CdSe)CdTe and (CdSe)ZnTe nanocrystals show that band warping is only significant in the highly strained structure (CdSe)CdTe, resulting in efficient recombination efficiency. (B) Representative transmission electron micrograph of a highly strained (CdSe)ZnS shows direct evidence of lattice warping at core-shell interfaces. Scale bar is 5 nm.